DOI: 10.1002/adma.200502556

Reversible Nanometer-Scale Data Storage on a Self-Assembled, Organic, Crystalline Thin Film**

By *Yongqiang Wen*, *Jingxia Wang*, *Junping Hu*, *Lei Jiang*, *Hongjun Gao*, *Yanlin Song*,* and *Daoben Zhu*

Information technology has revolutionized daily life in the last number of decades, and the continuously increasing amount of data to be stored and manipulated has strongly stimulated the search for switching and memory elements with sizes as small as a single molecule or even a single atom.[1] The invention of scanning tunneling microscopy (STM) has made it possible to bring this vision into reality. With the improvement of scanning probe microscopy (SPM) technology and the adoption of new functional materials, tremendous progress has been made in recent years in the development of SPM-based information storage.[2–5] For example, Cavallini et al. have achieved an areal density of 10–100 Gbits cm^{-2} based on the mechanical motion of rotaxane molecules using atomic fore microscopy (AFM);[2] by means of scanning near-field optical microscopy (SNOM), Labardi et al. have demonstrated optical read, write, and erase operations at the sub-micrometer-scale on azo-polymethacrylate thin films.[4]

Although the research on SPM-based storage has demonstrated great achievements, a number of technical challenges have to be effectively overcome. Future developments will aim at further reducing the bit size, decreasing the error rate, and increasing the data-storage rate. The improvement of the quality and intrinsic characteristics of the storage medium is one of the key points for solving these problems. From a practical viewpoint, the composing units of the storage media should be arranged in an ordered manner over a large area and the thin film should have a flat and stable surface. Compared with other materials, organic materials, which exhibit not only a controllable field-responsive character but also a favorable assembly capability, have shown unique predominance in the field of molecular electronics.[6]

Earlier, we designed complexes of (2,2-dimethyl-α,α,α′,α′-tetraphenyldioxolane-4,5-dimethanol) and coumarin (TAD-DOL-coumarin, TC) for SPM-based information storage.[7] By virtue of strong intermolecular interactions, we have successfully fabricated a TC supramolecular crystalline thin film and realized ultrahigh-density data storage.[7] However, analysis of the mechanism showed that, owing to the absence of reversible field-responsive groups in the molecules, the rupture of intermolecular hydrogen bonds was the main reason for the recording-dot formation, which led to an irreversible transformation on the film's surface. So, the study of ordered films with field-responsive characteristics became the main goal of our further efforts towards reversible data storage. Without doubt, donor–acceptor compounds or complex systems exhibiting electrical bistability due to field-induced reversible intermolecular charge transfer[8] are ideal sources of inspiration to design novel materials for reversible information storage.

In this communication, an organic donor–acceptor molecule, 4′-cyano-2,6-dimethyl-4-hydroxy azobenzene (CDHAB, Scheme 1) has been designed and synthesized for STM-based data storage. In a single CDHAB molecule, a hydroxyl group and a cyano group are included, which act not only as electron donor and acceptor groups, respectively, but also as hydrogen-bonding recognition subunits. Using molecular self-organization, CDHAB molecules have been assembled into a highly ordered crystalline thin film on a freshly cleaved, highly ordered pyrolytic graphite (HOPG) substrate. We have successfully realized reversible nanometer-scale data storage by STM on such thin films, and the change in conductance of the CDHAB film was the reason for the information-dot formation. This work represents a further step forward in improving the performance of storage media for SPM-based reversible information storage.

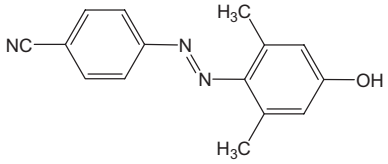

Scheme 1. Molecular structure of 4′-cyano-2,6-dimethyl-4-hydroxy azobenzene, CDHAB.

Drop-casting has been used for preparing CDHAB films. The quality and thickness of the films were controlled through the choice of solvents, their proportions, and concentrations. In a typical film-preparation process, a solution of CDHAB in

[*] Prof. Y. L. Song, Dr. Y. Q. Wen, Dr. J. X. Wang, Dr. J. P. Hu, Prof. L. Jiang, Prof. D. B. Zhu
Organic Solids Laboratory, Institute of Chemistry
Chinese Academy of Sciences, Beijing, 100080 (P.R. China)
E-mail: ylsong@iccas.ac.cn
Prof. H. J. Gao
Nanoscale Physics and Devices Laboratory, Institute of Physics
Chinese Academy of Sciences, Beijing 100080 (P.R. China)

[**] This work is supported by NSFC (Grant Nos. 50173028, 20574084, 90201036) and 863 Project (Grant No. 2002 AA302101, 2004AA302013). Supporting Information is available online from Wiley InterScience or from the author.

ADVANCED MATERIALS

a mixture of toluene and chloroform (5:1) with a concentration of about 5.0×10^{-5} mol L^{-1} was used, and the thin film was obtained by drop-casting on a HOPG substrate after complete solvent evaporation at room temperature. Figure 1A displays the AFM topographic image of the thin film on a HOPG substrate. The observed area is about 10.0 μm × 10.0 μm. The topography clearly illustrates the flat form of the thin film in micrometer-sized areas. By analyzing the cross section of the AFM scanning image (Supporting Information, Fig. S1), we have obtained a value of about 5 nm for the film thickness. In order to investigate the internal structure of the thin film, the transmission electron diffraction pattern (EDP) has been measured. Figure 1B displays the transmission electron microscopy (TEM) image of the thin film and its representative selected-area EDP (Fig. 1B, inset). As seen from Figure 1B, the TEM image shows a uniform and flat surface, and the EDP shows a fairly clear spot pattern, indicating the highly crystalline nature of the thin film.

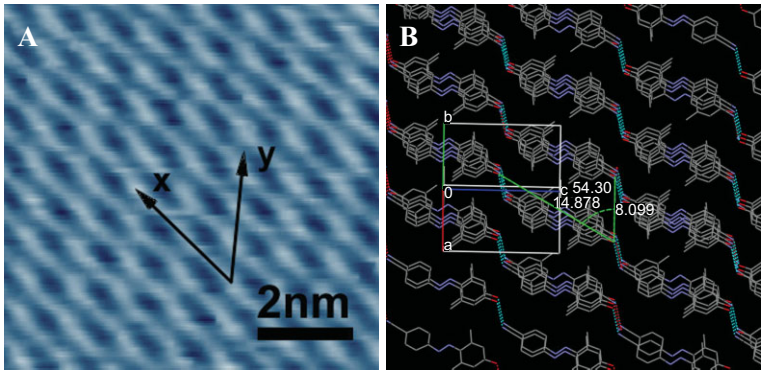

Figure 2. A) A typical STM image of a crystalline CDHAB thin film showing its crystalline order. Scanning conditions: bias voltage, $V_{bias} = 0.36$ V, reference current, $I_{ref} = 0.25$ nA. The periods along the *x*- and *y*-directions marked in the image are 1.5 and 0.8 nm, respectively, and the angle between them is 53°. B) A structural model to show the stacking arrangement of CDHAB molecules in the crystalline thin film. The periods along the long axis of a CDHAB molecule and between adjacent rows as well as the angle between them are 14.878 Å, 8.099 Å, and 54.30°, respectively.

Figure 2A shows a typical STM image of a CDHAB thin film, where the CDHAB molecules are arranged periodically on the HOPG substrate; the periodic distances along the *x*- and *y*-directions marked in the image are 1.5 and 0.8 nm, respectively, and the angle between them is 53°. These values are perfectly consistent with the periods along the long axis of CDHAB molecules and between adjacent rows of molecules, as well as the angle between these, as shown in the model of the stacking arrangement of CDHAB molecules in a bulk crystal (Fig. 2B).[9] Considering the structure of CDHAB, we can reasonably assume that the cooperative interaction effects of hydrogen bonding, π–π interactions, and van der Waals forces lead to the orderly arrangement of CDHAB molecules on the HOPG substrate.[10] Such a uniform, smooth thin film with suitably large, highly ordered regions is the basis for practical technological applications.

A flat region has been selected for the information recording experiments. To induce the recording dots, pulsed voltages of 0 to +6.0 V in amplitude and 0.01 to 10 ms in width were applied between the conductive probe and the crystalline thin film. To avoid running into the surface, the STM tip was lifted up several angstroms from the tunneling position and the feedback loop was disabled before applying a pulse voltage. By applying pulsed voltages of +2.6 V and 3.0 ms between the STM tip and the sample substrate, we succeeded in writing a letter-"y" pattern on the crystalline CDHAB thin film. Figure 3A shows the STM image of the recorded dot pattern in a scanning area of 60 nm × 60 nm. One bright dot corresponds to a recorded mark. The average dot size is about 1.8 nm in diameter. In our experiment, the recorded marks were very stable and no obvious changes could be observed during the continuous scanning process of 6 h. Further studies have shown that when the pulsed voltage was lower than a threshold of +2.6 V, no dots were recorded, but for voltage pulses

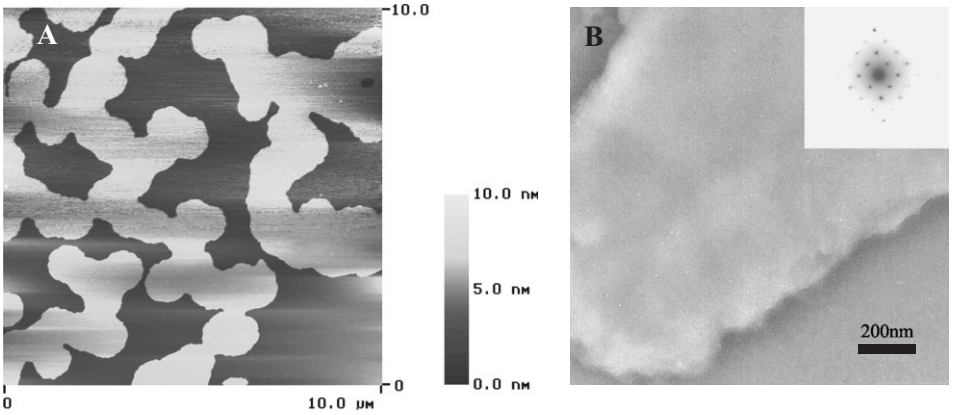

Figure 1. A) AFM image of a CDHAB thin film on HOPG prepared by self-assembly (area shown is 10.0 μm × 10.0 μm). B) Transmission electron microscopy (TEM) image of a CDHAB thin film and its electron diffraction pattern (EDP) in the inset.

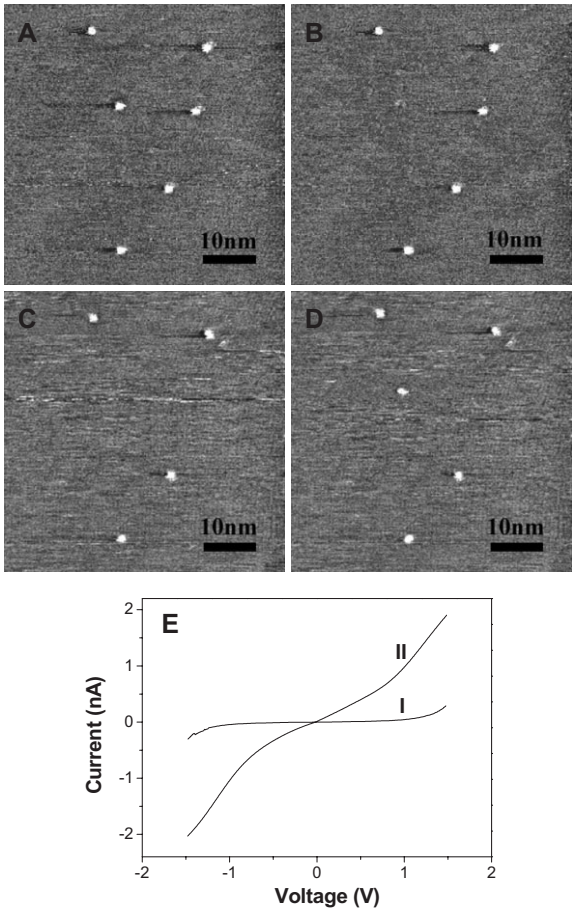

Figure 3. STM images of the CDHAB film during the information recording experiments. Tunneling conditions: $V_{bias} = 0.38$ V, $I_{ref} = 0.28$ nA, 0.2 Hz/image, constant-current mode. A) A recorded pattern (letter "y"), voltage pulses: +2.6 V, 3.0 ms; area shown is 60 nm × 60 nm. B,C) Patterns after erasing one and two marks, respectively, voltage pluses: –2.2 V, 3.0 ms. D) Pattern after rewriting one mark, voltage pulse: +2.6 V, 3.0 ms; E) typical STM current–voltage (*I–V*) curves in the unrecorded (curve I) and recorded region (curve II).

above the threshold, the probability of dot formation was almost 100 %. Furthermore, when a reverse-polarity voltage pulse higher than an absolute value of 2.2 V was applied to the recorded region, the marks could be erased. The images in Figure 3B and C indicate, respectively, the situation after one and two information dots have been erased. By applying a pulsed voltage on the same region of thin film again, a mark can be rewritten on it (Fig. 3D). With alternating exposure of the film to positive and negative voltages beyond the threshold value, more than ten write–read–erase cycles have been demonstrated in the same area.

The local electrical properties of CDHAB storage thin films reported here have been characterized by examining the current–voltage (*I–V*) characteristics using STM (Fig. 3E). From the curves it is clear that the CDHAB film shows a different conductance before and after formation of the information marks. As shown by curve I in Figure 3E, the tunneling current remains low in the CDHAB film in its initial state. After a pulse voltage higher than the threshold (+2.6 V), the film shows a low impedance during the same voltage conditions (curve II) at the recorded region.

Up to now, there have been many reports of threshold switching and memory phenomena in organic materials and metal–organic complexes, and their electrically bistable devices.[11–16] The underlying mechanisms include intermolecular charge transfer in organic donor–acceptor compounds or complexes,[8f,g] structural phase transitions,[11,14,15] and chemical changes in organic molecules.[16] In the present case, physical damage of the film can obviously be ruled out because of the storage reversibility. The *I–V* characteristics of the film before and after recording suggest that the formation of information dots is due to the electrical switching of the CDHAB film from a high-impedance state to a low-impedance state. It is reasonable to assume that such a conductance change might be caused by reversible intermolecular charge transfer, as has been frequently observed in other donor–acceptor compounds and complexes.[8]

To further validate this assumption, we have studied the conductive behavior of macroscopic CDHAB films and the corresponding characteristic spectra. For this study, a thin film about 200 nm thick was used. *I–V* curves measured on an indium tin oxide (ITO)-coated glass substrate are shown in Figure 4A. From curve I it has been found that when the applied voltage is low, the film shows a high-impedance state (OFF state). Beyond a threshold of about +2.8 V, an electrical transition from the high-impedance state to a low-impedance state (ON state) takes place with an abrupt increase in current. The film shows good stability in this high-conductivity state during the subsequent voltage scan (curve II). The high-conductivity state could be returned to the low-conductivity state (OFF state) by applying a negative bias, as indicated in curve III, where the current suddenly drops at –2.5 V. After the film has returned to the low-conductivity state, it can be kept at this state during a negative bias scan and can be switched back to the high-conductivity state by applying a positive bias higher than the threshold, resulting in an OFF–ON–OFF–ON reversible trait. The CDHAB film exhibits consistent electrical bistability under macroscopic conditions (as Fig. 3E indicates). Transient conductance measurements (Fig. S3, Supporting Information) performed on the same sample have shown a short transition time of about 45 ns. UV-vis spectra of a CDHAB thin film in two different electrically stable states were further compared. Figure 4B and C exhibits the UV-vis spectra before and after the action of an electrical field higher than the threshold voltage of +2.8 V, respectively. From the result, it can be seen clearly that, in addition to the intrinsic bands of the CDHAB film at 346 and 456 nm before the application of an electrical field (Fig. 4B), the spectrum of the CDHAB film after the application of an electrical field (Fig. 4C) exhibits two additional bands at 427 and 498 nm, indicating the intensive interaction among molecules, especially intermolecular charge transfer.[8g,17] When the film is switched back to the high-impedance state, the UV-vis spectrum shows the initial state again.

ADVANCED MATERIALS

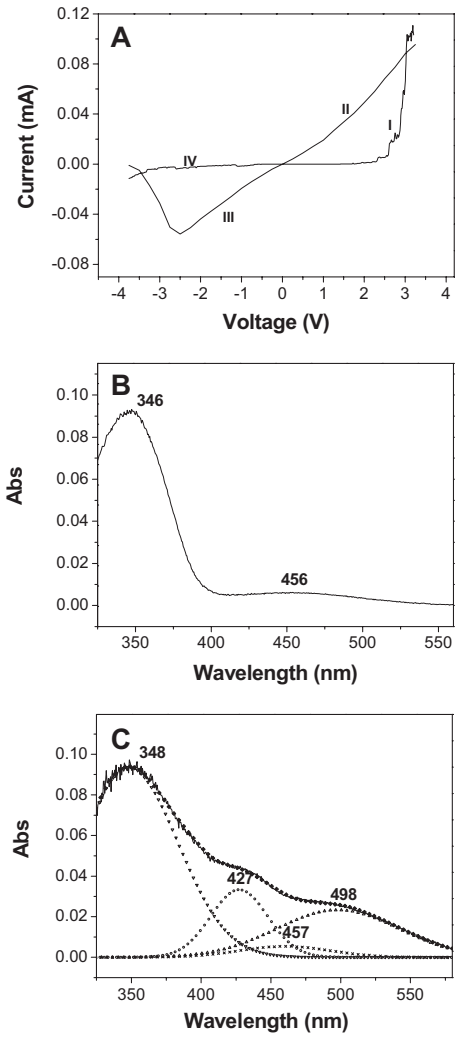

Figure 4. A) *I–V* characteristics of CDHAB films on ITO-coated glass, exhibiting the conductance transition from the low- to the high-conductivity state in curve I, the memory effect of the high-conductivity state in curve II, and the recovery of the low-conductivity state with the application of a reverse voltage scan in curves III and IV. UV-vis spectra of the CDHAB film before (B) and after (C) application of an electrical field higher than the threshold voltage of +2.8 V. The experimental spectra (solid line) is fitted (by the Gaussian peakfit method) with four components at 348 nm (▼), 427 nm (●), 457 nm (×), and 498 nm (▲) to give the combined signal (◆).

In conclusion, we have designed the molecule CDHAB and prepared its crystalline thin film by molecular self-assembly. Reversible nanometer-scale data storage was realized on such thin films by applying pulsed voltages between the STM tip and HOPG substrate. An analysis of the mechanism suggests that the formation of the recording dots is due to a local change of the film's electrical properties, and reversible intermolecular charge transfer induced by electric fields is proposed as the possible reason for that change. This result shows that the STM-based memory with a self-assembled donor–acceptor compound in a crystalline thin film is a promising candidate for realizing reversible nanometer-scale data storage.

Experimental

CDHAB was available by the azo coupling reaction [18] in 70 % yield; melting point, m.p. = 182 °C. Elemental analysis for $C_{15}H_{13}N_3O$: Calcd: C, 71.70; H, 5.21; N, 16.72. Found: C, 71.22; H, 5.76; N, 16.25. IR (KBr): ν_{max}=3371 (OH, str), 2230 (CN, str), 1599 (benzene ring, str), 1432 cm^{-1} (N=N, str). ^1H NMR (400 MHz $CDCl_3$): δ=7.89 (m, 2H, ArH), 7.78 (m, 2H, ArH), 6.63 (m, 2H, ArH), 2.52 ppm (s, 6H, $-CH_3$). ^{13}C NMR (400 MHz $CDCl_3$): δ=157.2, 155.2, 143.9, 137.1, 133.2, 122.7, 118.7, 116.3, 112.8, 20.7 ppm. Electrospray ionization mass spectroscopy (ESI-MS) *m/z*: 250.1 [M – H].

TEM images and EDP were collected with a Hitachi H-8100 TEM operated at 200 kV. Amorphous carbon thin films were adopted as supporting films. The information storage experiments and local *I–V* measurements were performed with a Solver P47 scanning probe microscope under ambient conditions, and electrochemically etched tungsten tips were used. Topographical characterization was performed with an SPI 3800N multimode scanning probe microscope (Seiko Instruments) in tapping mode with a silicon cantilever having a nominal spring constant of 3 $N\,m^{-1}$ and a resonant frequency of 24 kHz at a scan rate of 0.50 Hz. The macroscopic conductive behavior of CDHAB films was investigated by using a Keithley 4200–SCS system. A thin film with thickness of about 200 nm on ITO-coated glass and a two-terminal junction were used for *I–V* measurements [15]. A piece of HOPG was used as the top electrode. The junction area was 10 mm × 10 mm. This setup was also used for transient conductance measurements with the combination of a Tektronix TM515 FG 502 11 MHz functional generator. The UV-vis spectra of the CDHAB crystalline films before and after applying macroscopic electric fields were investigated with a Hitachi U4100 spectrophotometer.

Received: November 29, 2005
Final version: January 25, 2006
Published online: July 4, 2006

[1] D. M. Eigler, C. P. Lutz, W. E. Rudge, *Nature* **1991**, *352*, 600.
[2] M. Cavallini, F. Biscarini, S. León, F. Zerbetto, G. Bottari, D. A. Leigh, *Science* **2003**, *299*, 531.
[3] E. Eleftheriou, T. Antonakopoulos, G. K. Binnig, G. Cherubini, M. Despont, A. Dholakia, U. Dürig, M. A. Lantz, H. Pozidis, H. E. Rothuizen, P. Vettiger, *IEEE Trans. Magn.* **2003**, *39*, 938.
[4] M. Labardi, N. Coppede, L. Pardi, M. Allegrini, M. Giordano, S. Patane, A. Arena, E. Cefali, *Mol. Cryst. Liq. Cryst.* **2003**, *398*, 33.
[5] S. Naberhuis, *J. Magn. Magn. Mater.* **2002**, *249*, 447.
[6] a) D. L. Keeling, N. S. Oxtoby, C. Wilson, M. J. Humphry, N. R. Champness, P. H. Beton, *Nano Lett.* **2003**, *3*, 9. b) S. I. Stupp, V. LeBonheur, K. Walker, L. S. Li, K. E. Huggins, M. Keser, A. Amstutz, *Science* **1997**, *276*, 384.
[7] Y. Q. Wen, Y. L. Song, G. Y. Jiang, D. B. Zhao, K. L. Ding, W. F. Yuan, H. J. Gao, L. Jiang, D. B. Zhu, *Adv. Mater.* **2004**, *16*, 2018.
[8] a) C. W. Chu, J. Y. Ouyang, J. H. Tseng, Y. Yang, *Adv. Mater.* **2005**, *17*, 1440. b) W. Xu, G. R. Chen, R. J. Li, Z. Y. Hua, *Appl. Phys. Lett.* **1995**, *67*, 2241. c) M. Ouyang, S. M. Hou, H. F. Chen, K. Z. Wang, Z. Q. Xue, *Phys. Lett. A* **1997**, *235*, 413. d) K. Z. Wang, Z. Q. Xue, M. Ouyang, H. X. Zhang, C. H. Huang, *J. Mater. Sci. Lett.* **1996**, *15*, 977. e) M. Ouyang, S. M. Hou, H. F. Chen, K. Z. Wang, Z. Q. Xue, *Phys. Lett. A* **1997**, *235*, 413. f) G. Y. Jiang, T. Michinobu, M. Feng, Y. Q. Wen, S. X. Du, H. J. Gao, L. Jiang, Y. L. Song, F. Diederich, D. B. Zhu, *Adv. Mater.* **2005**, *17*, 2170. g) H. M. Wu, Y. L. Song, S. X. Du, H. W. Liu, H. J. Gao, L. Jiang, D. B. Zhu, *Adv. Mater.* **2003**, *15*, 1925.
[9] Crystal structure analysis of CDHAB: $C_{15}H_{13}N_3O$, relative molecular mass (M_r) = 251.29; space group triclinic *P*-1, *a* = 7.523(2), *b* = 8.099(2), *c* = 12.097(3) Å, α = 92.76(2)°, β = 91.68(2)°, γ = 116.72(2)°, *V* = 656.511(2) $Å^3$, *Z* = 2, ρ = 1.271 $g\,cm^{-3}$, μ = 0.08 mm^{-1}, *T* = 298 K, *R* = 0.0473, R_w = 0.0547. R. E. Marsh, *Acta Crystallogr., Sect. B: Struct.*

Sci. **1995**, *51*, 897. These data can be obtained free of charge from the Cambridge Crystallographic Data Centre (CCDC) via www.ccdc.cam.ac.uk/data_request/cif.

[10] a) J.-M. Lehn, *Supramolecular Chemistry: Concepts and Perspectives*, VCH, Weinheim, Germany **1995**. b) B. Moulton, M. J. Zaworotko, *Chem. Rev.* **2001**, *101*, 1629. c) C. G. Claessens, J. F. Stoddart, *J. Phys. Org. Chem.* **1997**, *10*, 254.

[11] R. S. Potember, T. O. Poehler, A. Rappa, *J. Am. Chem. Soc.* **1980**, *102*, 3659.

[12] M. Ouyang, S. M. Hou, H. F. Chen, K. Z. Wang, Z. Q. Xue, *Phys. Lett. A* **1997**, *235*, 413.

[13] M. Matstumoto, *Chem. Lett.* **1991**, *6*, 1021.

[14] H. J. Gao, K. Sohlberg, Z. Q. Xue, H. Y. Chen, S. M. Hou, L. P. Ma, X. W. Fang, S. J. Pang, S. J. Pennycook, *Phys. Rev. Lett.* **2000**, *84*, 1780.

[15] M. Feng, X. F. Guo, X. Lin, X. B. He, W. Ji, S. X. Du, D. Q. Zhang, D. B. Zhu, H. J. Gao, *J. Am. Chem. Soc.* **2005**, *127*, 15 338.

[16] D. X. Shi, Y. L. Song, H. X. Zhang, P. Jiang, S. T. He, S. S. Xie, S. J. Pang, H. J. Gao, *Appl. Phys. Lett.* **2000**, *77*, 3203.

[17] a) H. A. Staab, C. P. Herz, C. Krieger, M. Rentea, *Chem. Ber.* **1983**, *116*, 3813. b) H. Oerhoeven, M. N. Paddon-Row, M. Heppener, A. M. Oliver, E. Cotsanies, J. W. Verhoeven, N. S. Hush, *J. Am. Chem. Soc.* **1987**, *109*, 3258. c) D. V. Lopatin, V. V. Rodaev, A. V. Umrikhin, D. V. Konarev, A. L. Litvinov, R. N. Lyubovskaya, *J. Mater. Chem.* **2005**, *15*, 657. d) J. P. Ni, Y. Ueda, *Mol. Cryst. Liq. Cryst.* **1999**, *337*, 289.

[18] K. Haghbeen, E. W. Tan, *J. Org. Chem.* **1998**, *63*, 4503.

